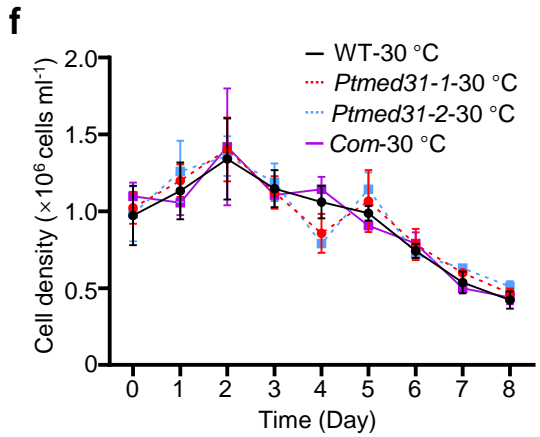
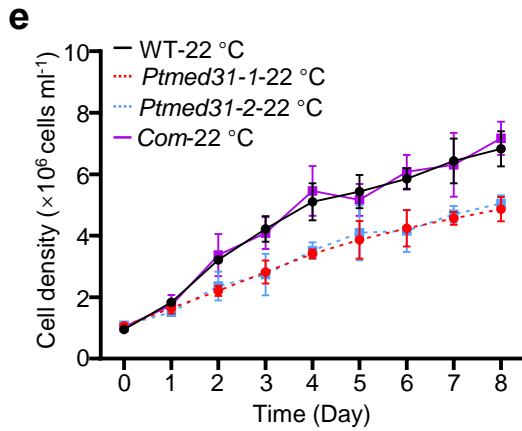
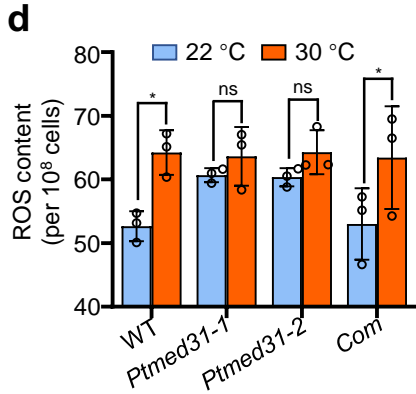
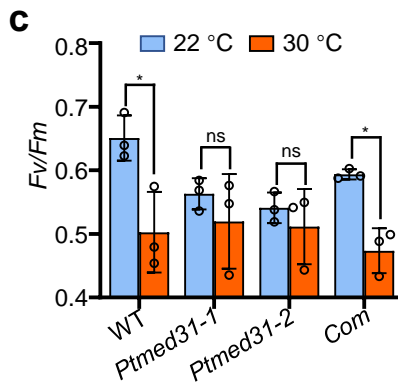
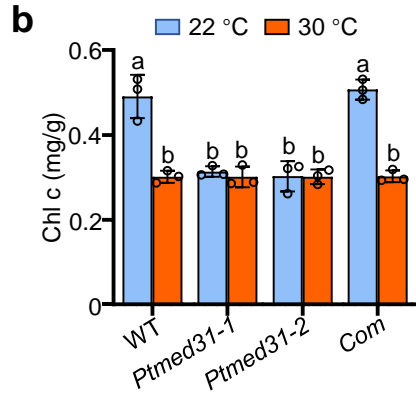
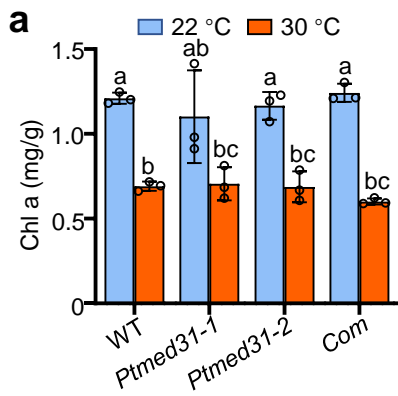
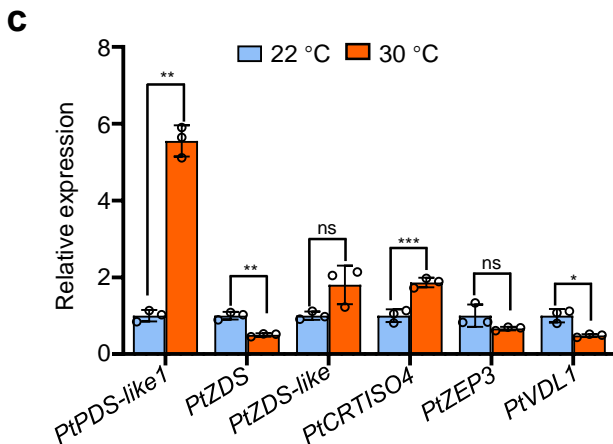
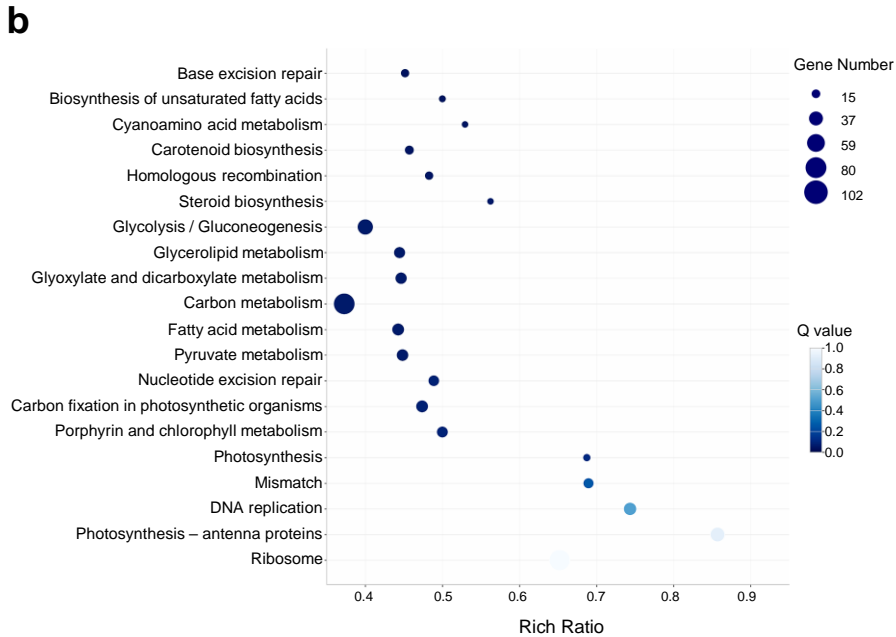
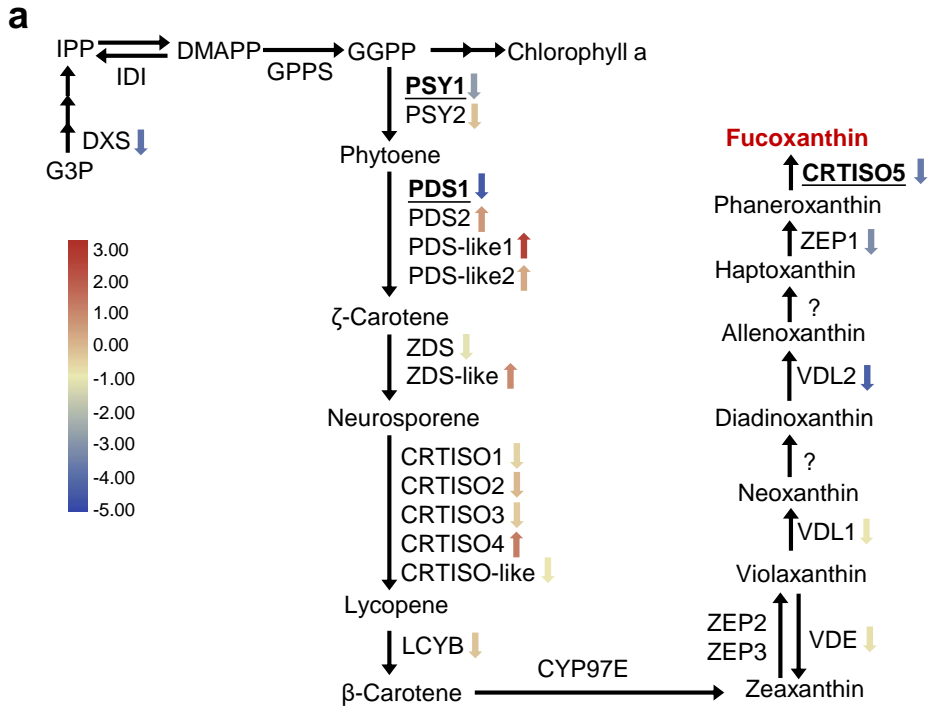


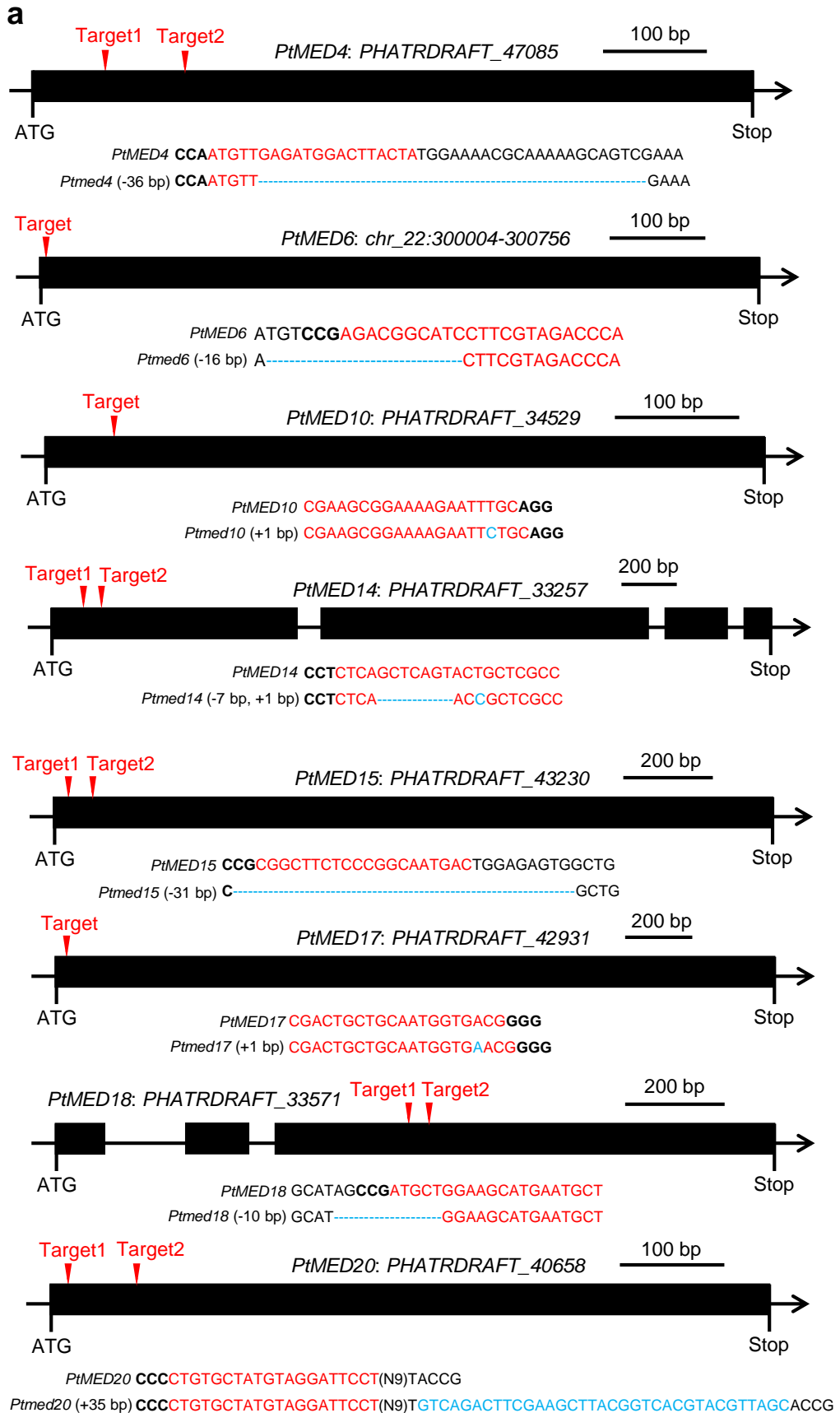
A proteolysis-dependent Mediator switch controls heat-responsive fucoxanthin biosynthesis in diatoms

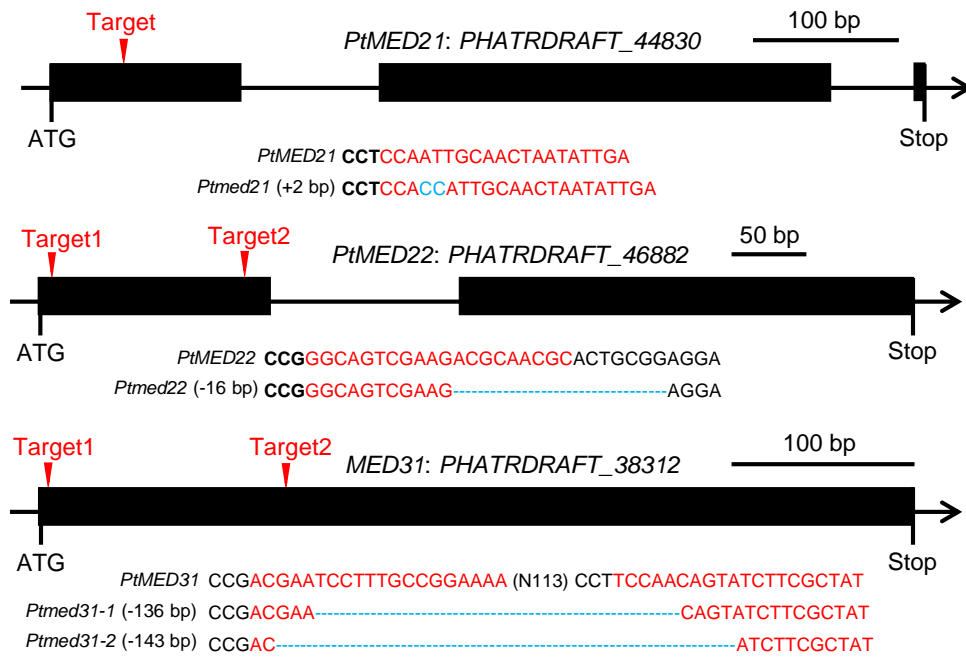
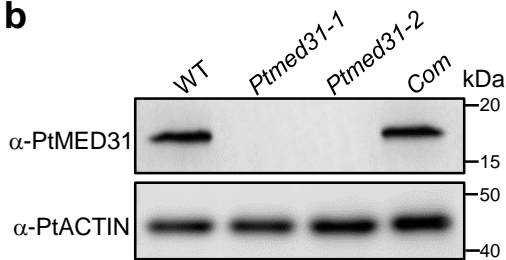
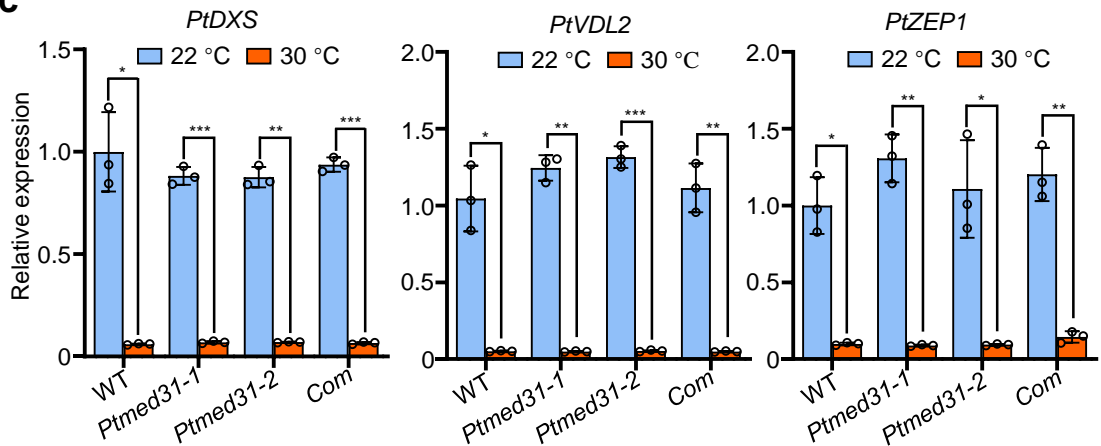


Supplementary Fig. 1 | PtMED31 contributes to photosynthetic pigment accumulation and photophysiological performance under normal and heat stress conditions. a,b Chlorophyll a (**a**) and chlorophyll c (**b**) contents of indicated lines at 22 °C and 30 °C. **c** Maximum quantum yield of photosystem II (PSII), measured as *Fv/Fm*, in the indicated lines at 22 °C and 30 °C. **d** Reactive oxygen species (ROS) levels in the indicated lines at 22 °C and 30 °C. **e,f** Time-course analysis of cell density in the indicated cell lines at 22 °C (**e**) and 30 °C (**f**). Data are presented as mean \pm SD from three independent biological replicates. In (**a**, **b**), different letters indicate significant differences among groups at $P < 0.05$. In (**c**, **d**), statistical significance was determined using Student's *t*-test between 22 °C and 30 °C within each line. * $P < 0.05$; ns, not significant.

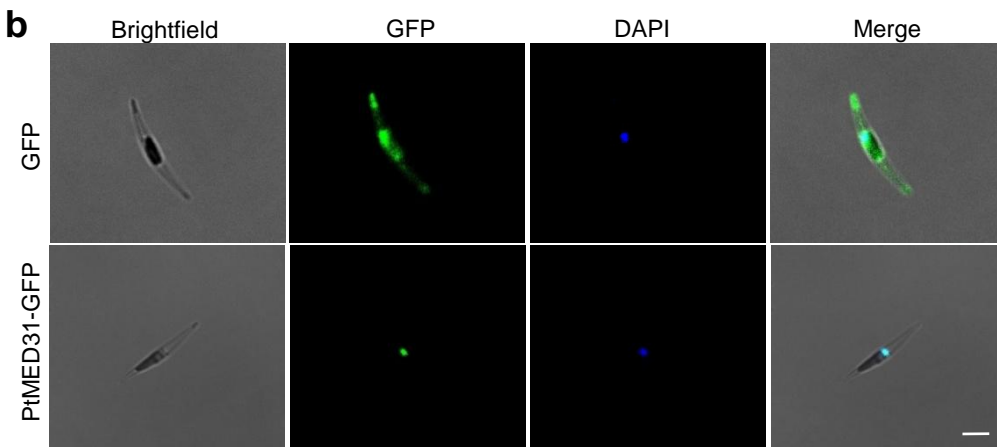
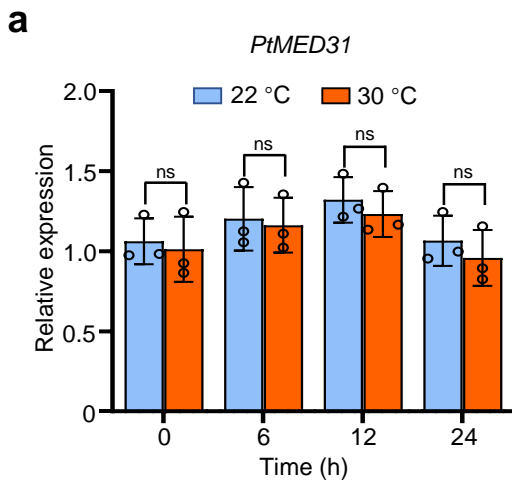


Supplementary Fig. 2 | Transcriptomic profiling of heat-repressed fucoxanthin biosynthesis and validation of selected genes by RT-qPCR. **a** Fucoxanthin biosynthetic pathway and transcriptomic changes in pathway-related genes in WT *P. tricornutum* under heat stress. The \log_2 fold changes in gene expression (30 °C vs 22 °C) in wild-type *P. tricornutum* are depicted by colored arrows positioned adjacent to each gene name. Genes exhibiting upregulation and downregulation are denoted by upward and downward arrows, respectively. **b** Top 20 enriched KEGG pathways identified from differentially expressed genes under heat stress. The y-axis denotes KEGG pathway terms, and the x-axis represents the rich ratio. Bubble size indicates the number of enriched genes, and bubble color represents the Q value, with lower Q values indicating greater statistical significance. **c** RT-qPCR validation of selected fucoxanthin-biosynthetic genes, including *PtPDS-like1*, *PtZDS*, *PtZDS-like*, *PtCRTISO4*, *PtZEP3*, and *PtVDL1*, in WT *P. tricornutum* cells incubated at 22 °C or 30 °C for 24 h before RNA extraction. Data are presented as mean \pm SD from three independent biological replicates, * $P < 0.05$, ** $P < 0.01$, *** $P < 0.001$ (Student's *t* test).

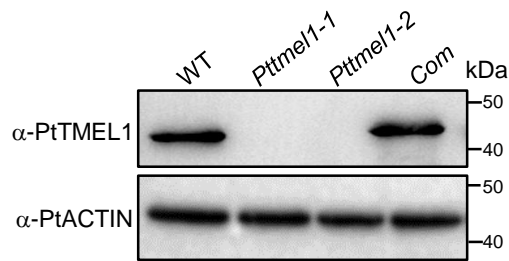


a**b****c**

Supplementary Fig. 3 | Generation and molecular characterization of CRISPR/Cas9-edited *Ptmed* mutant lines. **a** Schematic diagrams showing CRISPR/Cas9 target sites and representative edited alleles of the indicated *PtMED* genes. Coding regions were targeted using specific sgRNAs. sgRNA target sequences are shown in red, and PAM sequences are shown in bold. Blue dashes indicate deletions, and blue letters indicate insertions. Numbers in parentheses indicate the sizes of insertions or deletions; +, insertion; -, deletion. **b** Immunoblotting analysis of PtMED31 protein abundance in WT, two independent *Ptmed31* mutant lines, and the *PtMED31*-complemented line. PtMED31 was detected using an anti-PtMED31 antibody, and PtACTIN was used as a loading control. **c** RT-qPCR analysis of the relative transcript levels of *PtDXS* (left), *PtVDL2* (middle), and *PtZEP1* (right) in the indicated lines incubated at 22 °C and 30 °C for 24 h before RNA extraction. In **c**, data are presented as mean \pm SD from three independent biological replicates. Statistical significance was determined using Student's *t*-test. **P* < 0.05, ***P* < 0.01, ****P* < 0.001.

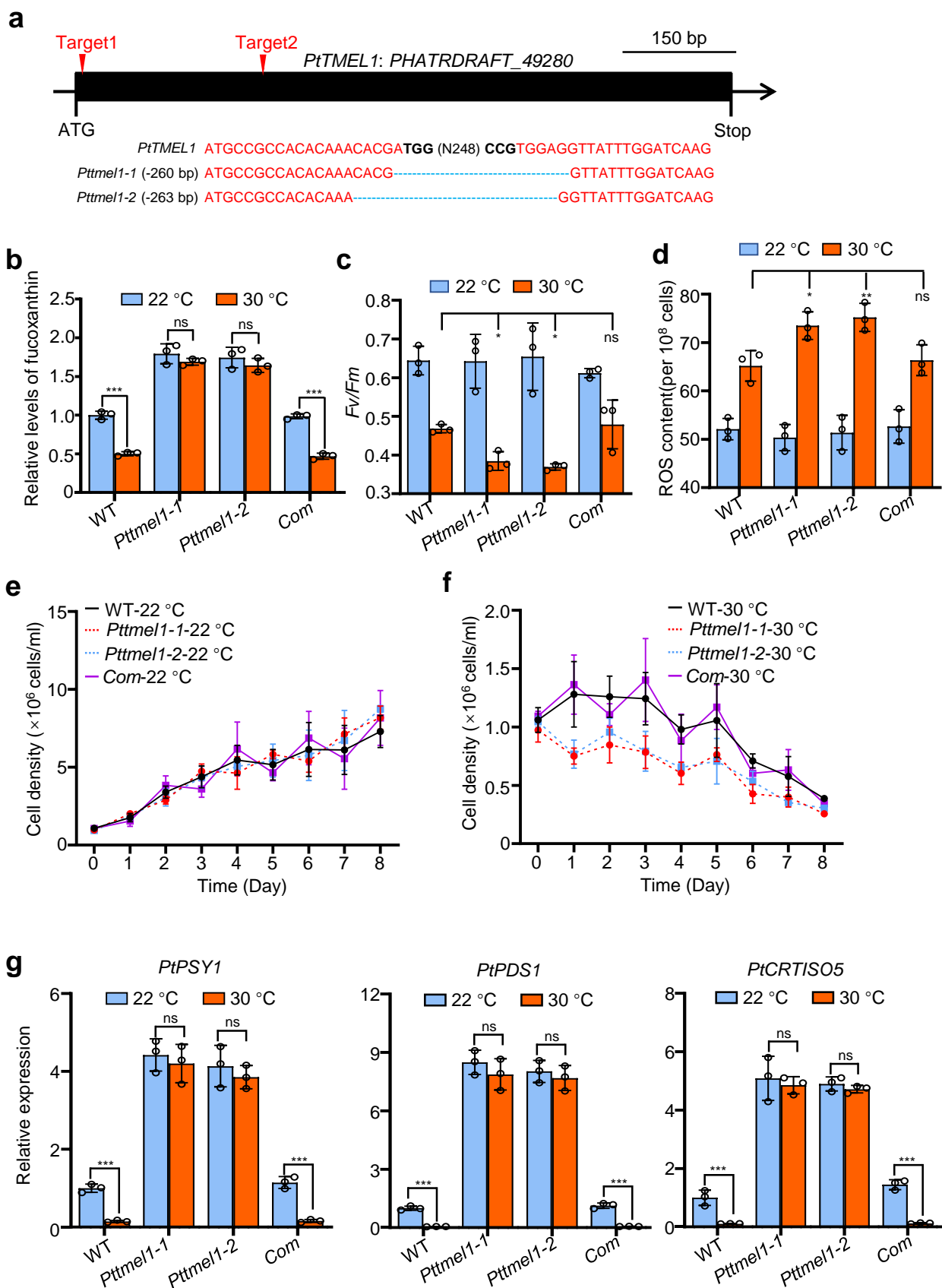


Supplementary Fig. 4 | Transcript abundance and subcellular localization of *PtMED31*. **a** RT-qPCR showing the *PtMED31* mRNA levels in WT at 22 °C and 30 °C for the indicated times. Data are presented as mean \pm SD from three independent biological replicates. Statistical significance was determined using Student's *t*-test between the 22 °C and 30 °C treatments at each time point; ns, not significant. **b** Representative fluorescence microscopy images showing the subcellular localization of PtMED31-GFP. DAPI was used to stain nuclei. Scale bar, 5 μ m.

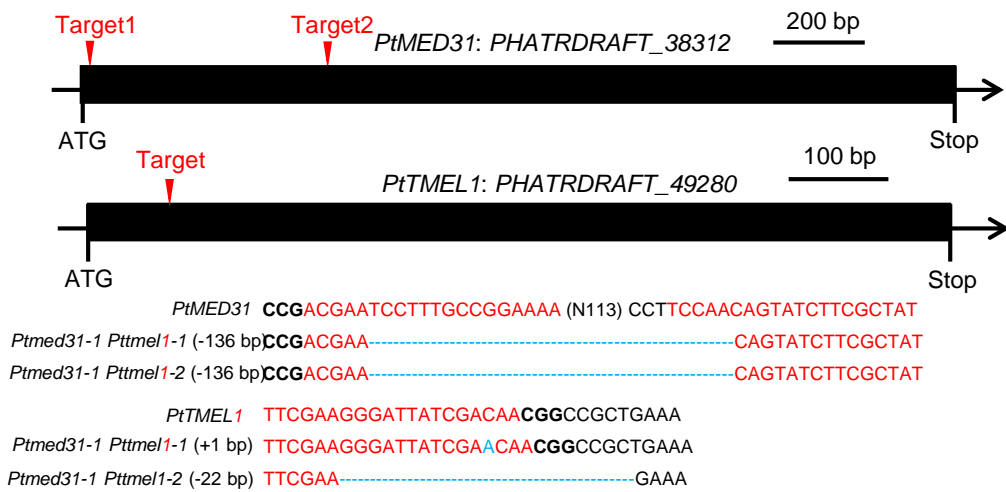


Supplementary Fig. 5 | Specificity validation of the anti-PtTMEL1 antibody.

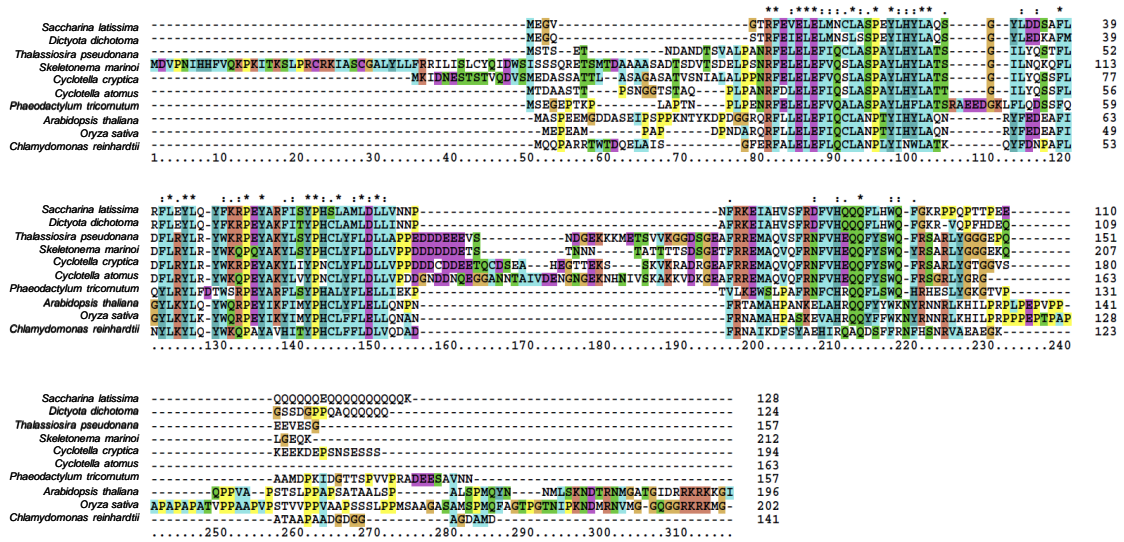
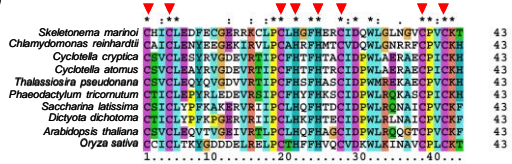
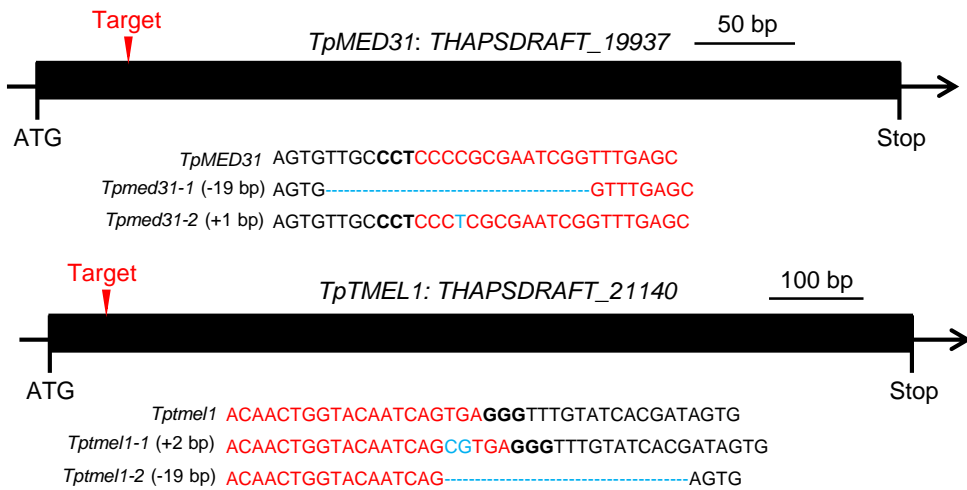
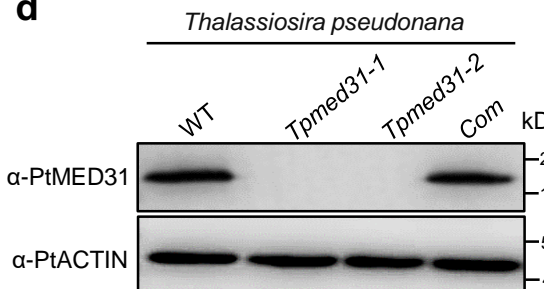
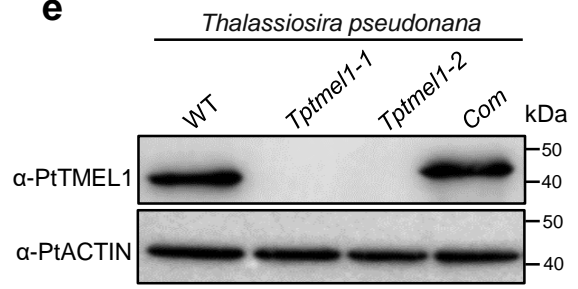
Immunoblotting analysis of PtTMEL1 protein abundance in WT, the *Pttmel1* mutant, and the *PtTMEL1*-complemented line (*Com*). Endogenous PtTMEL1 was detected using an anti-PtTMEL1 antibody, and PtACTIN was used as a loading control. The immunoblot is representative of three independent experiments.



Supplementary Fig. 6 | Generation and characterization of *Pttmel1* mutant and complemented lines. **a** Schematic diagram showing CRISPR/Cas9-mediated editing of the *PtTMEL1* locus. Two sgRNAs were designed to target the coding region of *PtTMEL1*. sgRNA target sequences are shown in red, and PAM sequences are shown in bold. Blue dashes indicate deletions. Numbers in parentheses indicate deletion sizes. **b** Relative fucoxanthin levels in WT, two independent *Pttmel1* mutant lines, and the *PtTMEL1*-complemented line at 22 °C and 30 °C. **c** Maximum quantum yield of PSII, measured as *Fv/Fm*, in the indicated lines at 22 °C and 30 °C. **d** ROS levels in the indicated lines at 22 °C and 30 °C. **e,f** Time-course analysis of cell density in the indicated lines at 22 °C (**e**) and 30 °C (**f**). **g** RT-qPCR analysis of the relative transcript levels of *PtPSY1* (left), *PtPDS1* (middle), and *PtCRTISO5* (right) in the indicated lines at 22 °C and 30 °C for 24 h before RNA extraction. In (**b-g**), data are presented as mean \pm SD from three independent biological replicates. * $P < 0.05$, *** $P < 0.001$ (Student's *t* test); ns, not significant.



Supplementary Fig. 7 | Generation and genotyping of *Ptmed31-1 Pttmel1* double-mutant lines. Schematic diagram showing CRISPR/Cas9-edited alleles at the *PtMED31* and *PtTMEL1* loci. The *Ptmed31-1 Pttmel1* double-mutant lines were generated in the *Ptmed31-1* mutant background by further editing the *PtTMEL1* coding region. The *Ptmed31-1* allele carried the original deletion at the *PtMED31* locus, whereas the *PtTMEL1* coding region was targeted using a single sgRNA. sgRNA target sequences are shown in red, and PAM sequences are shown in bold. Blue dashes indicate deletions, and blue letters indicate insertions. Numbers in parentheses indicate the sizes of insertions or deletions; +, insertion; -, deletion.

a**b****c****d****e**

Supplementary Fig. 8 | Conservation of MED31 and the TMEL1 RING domain and generation of *Tpmed31* and *Tptmel1* mutant lines. **a** Alignment of MED31 proteins among different species using the ClustalX2 software (version, 2.1). Conserved residues are highlighted according to the ClustalX color scheme. **b** Alignment of RING domain of TMEL1 among different species using the ClustalX2 software (version, 2.1). Arrowheads indicate conserved cysteine and histidine in C3H2C3-type RING-H2 finger consensus motif (C-X2-C-X(9-39)-C-X(1-3)-H-X(2-3)-H-X2-C-X(4-48)-C-X2-C). **c** Schematic diagrams showing CRISPR/Cas9-mediated editing of the *TpMED31* and *TpTMEL1* loci. The coding regions of *TpMED31* and *TpTMEL1* were each targeted using a single sgRNA. sgRNA target sequences are shown in red, and PAM sequences are shown in bold. Blue dashes indicate deletions, and blue letters indicate insertions. Numbers in parentheses indicate the sizes of insertions or deletions; +, insertion; -, deletion. **d** Immunoblotting analysis of TpMED31 protein abundance in WT, two independent *Tpmed31* mutant lines, and the *TpMED31*-complemented line (*Com*). TpMED31 was detected using an anti-PtMED31 antibody that cross-reacts with TpMED31. **e** Immunoblotting analysis of TpTMEL1 protein abundance in WT, two independent *Tptmel1* mutant lines, and the *TpTMEL1*-complemented line (*Com*). TpTMEL1 was detected using an anti-PtTMEL1 antibody that cross-reacts with TpTMEL1. In (**d,e**), ACTIN was used as a loading control.